



Research Article

# Catalytic Performance of TiO<sub>2</sub>-Carbon Mesoporous-Derived from Fish Bones in Styrene Oxidation with Aqueous Hydrogen Peroxide as an Oxidant

Mukhamad Nurhadi<sup>1,\*</sup>, Ratna Kusumawardani<sup>1</sup>, Teguh Wirawan<sup>2</sup>, S. Sumari<sup>3</sup>, Sin Yuan Lai<sup>4</sup>, Hadi Nur<sup>5,6</sup>

<sup>1</sup>Department of Chemical Education, Universitas Mulawarman, Kampus Gunung Kelua, Samarinda, 75119, East Kalimantan, Indonesia.

<sup>2</sup>Chemistry Department, Universitas Mulawarman, Kampus Gunung Kelua, Samarinda, 75119, East Kalimantan, Indonesia.

<sup>3</sup>Chemistry Department, Universitas Negeri Malang, Jl Semarang 5, Malang, 65145, Indonesia.

<sup>4</sup>School of Energy and Chemical Engineering, Xiamen University Malaysia, Selangor Darul Ehsan 43900, Malaysia and College of Chemistry and Chemical Engineering, Xiamen University, Xiamen 361005, China.

<sup>5</sup>Center for Sustainable Nanomaterials, Ibnu Sina Institute for Scientific and Industrial Research, Universiti Teknologi Malaysia, Johor Bahru, 81310, Malaysia.

<sup>6</sup>Central Laboratory of Minerals and Advanced Materials, Faculty of Mathematics and Natural Sciences, State University of Malang, Indonesia.

Received: 10<sup>th</sup> December 2020; Revised: 3<sup>rd</sup> February 2021; Accepted: 4<sup>th</sup> February 2021

Available online: 25<sup>th</sup> February 2021; Published regularly: March 2021



## Abstract

The catalytic performance of titania-supported carbon mesoporous-derived from fish bones (TiO<sub>2</sub>/CFB) has been investigated in styrene oxidation with aqueous H<sub>2</sub>O<sub>2</sub>. The preparation steps of (TiO<sub>2</sub>/CFB) catalyst involved the carbonization of fish bones powder at 500 °C for 2 h. followed by impregnation of titania using titanium(IV) isopropoxide (500 μmol) precursor, and calcined at 350 °C for 3 h. The physical properties of the adsorbents were characterized using Fourier transform infrared, X-ray diffraction (XRD), Scanning electron microscopy with energy dispersive X-ray (SEM-EDX), and nitrogen adsorption-desorption studies. The catalytic test was carried out using styrene oxidation with H<sub>2</sub>O<sub>2</sub> as an oxidant at room temperature for 24 h. Its catalytic activity was compared with Fe<sub>2</sub>O<sub>3</sub>/CFB, CuO/CFB, TiO<sub>2</sub>, and CFB catalysts. It is demonstrated that the catalytic activity of TiO<sub>2</sub>/CFB catalyst has the highest compared to Fe<sub>2</sub>O<sub>3</sub>/CFB, CuO/CFB, TiO<sub>2</sub>, and CFB catalysts in the oxidation of styrene with styrene conversion ~23% and benzaldehyde selectivity ~90%. Kinetics of TiO<sub>2</sub>/CFB catalyzed oxidation of styrene has been investigated and mechanism for oxidation of styrene has been proposed.

Copyright © 2021 by Authors, Published by BCREC Group. This is an open access article under the CC BY-SA License (<https://creativecommons.org/licenses/by-sa/4.0>).

**Keywords:** Titania; Fish bones; Carbon; Oxidation; Styrene; Hydrogen peroxide

**How to Cite:** M. Nurhadi, R. Kusumawardani, T. Wirawan, S. Sumari, S.Y. Lai, H. Nur (2021). Catalytic Performance of TiO<sub>2</sub>-Carbon Mesoporous-Derived from Fish Bones in Styrene Oxidation with Aqueous Hydrogen Peroxide as an Oxidant. *Bulletin of Chemical Reaction Engineering & Catalysis*, 16(1), 88-96 (doi:10.9767/bcrec.16.1.9729.88-96)

**Permalink/DOI:** <https://doi.org/10.9767/bcrec.16.1.9729.88-96>

## 1. Introduction

Styrene oxidation is one of the vital reactions in the oxidation of olefin for the production of

various fine chemicals, such as: benzaldehyde, phenyl acetaldehyde, and styrene epoxide. Benzaldehyde produced in this reaction has attracted interest due to this compound is used for the production of perfumes, pharmaceuticals, and agrochemicals [1]. Oxidation styrene with hydrogen peroxide as an oxidant is highly

\* Corresponding Author.

Email: nurhadi1969@yahoo.co.id (M. Nurhadi);

Telp.: +62 81346482251; Fax: +62 541 743929

advocated, because it is bestowed with advantages, such as: an environmentally friendly, high atom economy, and only water as the by-product. Many heterogeneous catalysts have been developed to increase yield product in styrene oxidation with  $\text{H}_2\text{O}_2$ . Multifarious efforts have been taken, including metal-supported mesoporous materials [2–6], metal-supported carbon material [7,8] and single-component metal oxides such as  $\text{Fe}_2\text{O}_3$  [9] and  $\text{Fe}_3\text{O}_4$  [10]. However, those catalysts, in general, involve complicated preparation methods, high production costs, and environmentally unfriendly.

Titanium dioxide ( $\text{TiO}_2$ ) or titania is a very well-researched materials catalysts that exhibit high efficiency in the oxidation reaction due to the stability of its chemical structure, biocompatibility, physical, optical and electrical properties. In nature, titania can be found in four polymorphs minerals form such as rutile, anatase, and brookite and titanium dioxide (B) or  $\text{TiO}_2(\text{B})$  [11,12]. Anatase and rutile were commonly used in the oxidation reaction due to commercial availability, large amounts of reactive oxygen species like hydroxyl ( $\cdot\text{OH}$ ) radicals, hydroperoxy radicals ( $\cdot\text{OOH}$ ) and superoxide ( $\cdot\text{O}_2^-$ ) radical anion onto  $\text{TiO}_2$  surface [1]. However, titania has low product yields if it is used without supported by catalyst support [13,14].

A support or a carrier is the inert substance that spreading out an expensive catalyst ingredient for its most effective use, expressly, the supports allow catalysts deposition or distribution homogeneously onto their surface, thus maximizing the number of catalytic active sites for reactions. Carbon can be considered as the potential catalyst supports, which can be used for catalyst reaction, but the support itself is nonreactive [6]. Waste from fish bones can be used as a particular alternative precursor for producing mesoporous carbon with a straightforward method [15].

Herein, we have developed a heterogeneous oxidation catalyst, a combination of titania as an active catalytic site and carbon mesoporous-derived fishbone as catalyst support. This catalyst system, titania supported carbon mesoporous-derived fishbone, has advantages such as cheaper, non-toxic, and environmentally friendly. The catalytic performance of this system was compared to the other transition metals supported carbon derived fish bones such as iron ( $\text{Fe}_2\text{O}_3$ ) and copper. The oxidation styrene with aqueous  $\text{H}_2\text{O}_2$  as an oxidant was used as a model reaction.

## 2. Materials and Methods

### 2.1 Carbonization Process

The waste of fish bones was collected from many food companies around Samarinda, East Kalimantan, Indonesia. The fish bone was washed with boiling water to remove impurities. Then, it was dried in the oven at  $110\text{ }^\circ\text{C}$  overnight. The dried fish bone was crushed to powder and carbonized in a furnace at  $500\text{ }^\circ\text{C}$  for 2 h. The carbon-derived from fish bone is labeled as CFB.

### 2.2 Titania Impregnation

One gram CFB was immersed in 10 mL toluene (Merck) that containing titanium(IV) isopropoxide (500  $\mu\text{mol}$ , Sigma Aldrich) and stirred until all of the toluene solvent completely evaporated. The sample was washed with ethanol (Merck) to remove the residual toluene and subsequently dried at  $110\text{ }^\circ\text{C}$  overnight. Then the sample was calcined at  $350\text{ }^\circ\text{C}$  for 2 h. The carbon of fish bone, which has been impregnated was labeled as  $\text{TiO}_2/\text{CFB}$ . As a comparison, 1 g samples were impregnated by copper nitrate trihydrate (500  $\mu\text{mol}$ , 10 mL, Merck) and Iron (III) nitrate nonahydrate (500  $\mu\text{mol}$ , 10 mL, Sigma Aldrich). Furthermore, both samples were calcined at  $350\text{ }^\circ\text{C}$  for 2 h, and the catalysts were notated as  $\text{CuO}/\text{CFB}$  and  $\text{Fe}_2\text{O}_3/\text{CFB}$ .

### 2.3 Catalysts Characterizations

The functional groups in the catalyst were identified by using the FTIR spectrometer (IR–Prestige–21 Shimadzu). The XRD (Phillips PANalytical X'Pert PRO type) was used to investigate the crystallinity and phase content of the catalyst with the  $\text{Cu K}\alpha$  ( $\lambda = 1.5406\text{ \AA}$ ) radiation and range of  $2\theta$  ( $^\circ$ ) from 7 to 60. The surface morphology of the catalyst was investigated by using SEM images obtained from a FEI Inspect S50 instrument. The surface area, pore-volume, and pore size distribution were determined by nitrogen adsorption-desorption isotherms that were created from the data collected from a Quantachrome nova 1200e instrument.

### 2.4 Catalytic Activity Test

Catalytic activity of the catalysts was carried by styrene (Merck) oxidation reaction with aqueous hydrogen peroxide ( $\text{H}_2\text{O}_2$  30%, Merck) as an oxidant. The catalytic reactions were carried out with a similar procedure reported pre-

viously [13,14,16]. All reactions were performed with mixing styrene (5 mmol), 30 % aqueous  $H_2O_2$  (5 mmol), acetonitrile (4.5 mL), and catalyst (50 mg) with stirring for 24 h at room temperature. The GC-2014 Shimadzu was used to analyze the product of the reaction.

### 3. Results and Discussions

#### 3.1 Physical Properties of Catalysts

Figure 1 shows the FTIR spectra of (a) CFB, (b) CuO, (c)  $Fe_2O_3$ , (d)  $TiO_2$ , (e)  $Fe_2O_3/CFB$ , (f) CuO/CFB and (g)  $TiO_2/CFB$ . The IR spectra of CFB show the absorption peaks at  $3436\text{ cm}^{-1}$ , and  $1632\text{ cm}^{-1}$  which indicating the O–H stretching. The C–O stretching vibration, which correlated to carbonate ion ( $CO_3^{2-}$ ) substitution in the crystal lattice, was investigated by the absorption bands at  $1435\text{ cm}^{-1}$  and  $877\text{ cm}^{-1}$  [17,18]. The absorption bands at  $1063\text{ cm}^{-1}$  and  $564\text{ cm}^{-1}$  are assigned to the P–O stretching vibration in phosphate ion ( $PO_4^{3-}$ ) groups [17,18]. The appearance of carbonate ion ( $CO_3^{2-}$ ) and phosphate ion ( $PO_4^{3-}$ ) groups are the evidence of the presence of hydroxyap-

atite. In the  $Fe_2O_3/CFB$ , CuO/CFB, and  $TiO_2/CFB$  catalysts, hydroxyapatite was assigned by the absorption band  $1094\text{ cm}^{-1}$  and  $591\text{ cm}^{-1}$ , which indicated the P–O stretching vibration in phosphate ion ( $PO_4^{3-}$ ) groups. The O–H stretching was investigated by the absorption band at  $672\text{ cm}^{-1}$ . After the impregnation of metal (Fe, Cu, Ti) and followed by the calcination process, the absorption band at  $3436\text{ cm}^{-1}$  [17,18], which indicated as O–H stretching, was drastically decreasing. The IR spectra of (b) CuO, (c)  $Fe_2O_3$  and (d)  $TiO_2$  were used to identify Cu, Fe and Ti in the samples. The metals of Cu and Fe can be identified by Cu–O and Fe–O vibration with absorption peaks at  $601$  and  $631\text{ cm}^{-1}$ , respectively. The existence of Ti framework was investigated by Ti–O vibration with an absorption broad peak at  $700\text{--}950\text{ cm}^{-1}$ . The metals of Cu, Fe, and Ti are no detected in the IR spectra 1 (e-g) due to the amount of metal that impregnated so small.

The XRD pattern in Figure 2 illustrates that the crystallinity of (a) CuO, (b)  $Fe_2O_3$ , (c)  $TiO_2$ , (d) CFB, (e)  $Fe_2O_3/CFB$ , (f) CuO/CFB,

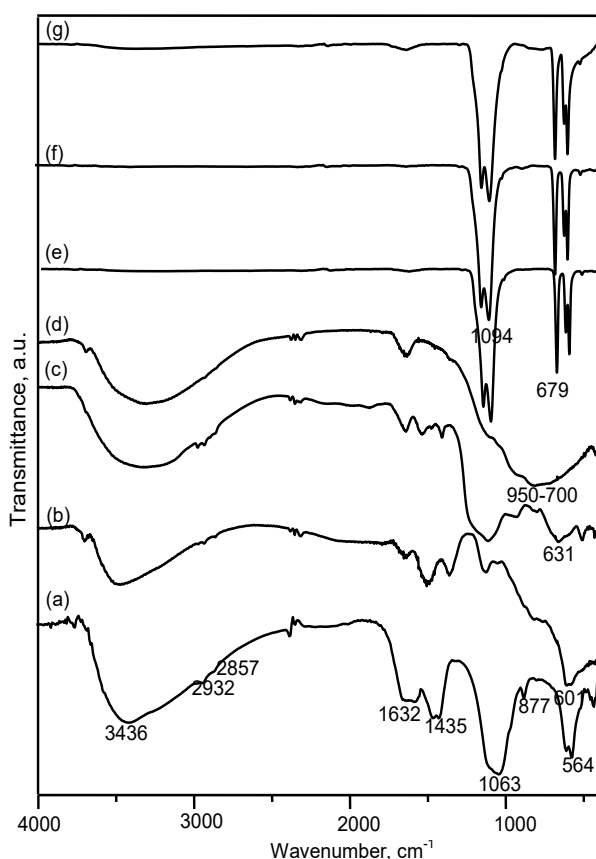


**Figure 1.** FTIR spectra of (a) CFB, (b) CuO, (c)  $Fe_2O_3$ , (d)  $TiO_2$ , (e)  $Fe_2O_3/CFB$ , (f) CuO/CFB and (g)  $TiO_2/CFB$ .

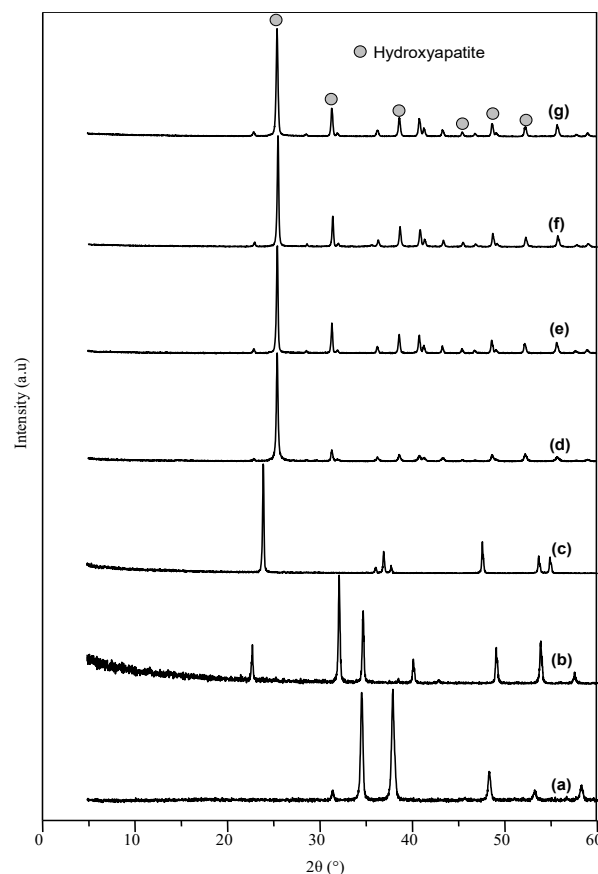


**Figure 2.** XRD pattern of (a) CuO, (b)  $Fe_2O_3$ , (c)  $TiO_2$ , (d) CFB, (e)  $Fe_2O_3/CFB$ , (f) CuO/CFB and (g)  $TiO_2/CFB$ .

and (g) TiO<sub>2</sub>/CFB catalysts. The CFB shows the low crystallinity, but otherwise, the high crystallinity was shown by Fe<sub>2</sub>O<sub>3</sub>/CFB, CuO/CFB and TiO<sub>2</sub>/CFB catalysts. Based on JCPDS 0760694, all catalysts contain hydroxyapatite, which proven by the diffraction peaks at 2θ = 25.9, 31.8, 46.8, 49.6, and 53.4. Based on JCPDS number 00-004-0477, the dominant diffraction peaks should be appeared at 2θ = 33.5 and 35.6 for Fe<sub>2</sub>O<sub>3</sub>; 35.5 and 38.9 for CuO and

25.2, 37.7 and 47.9 for TiO<sub>2</sub>, but it did not appear in Figure 2 (e-g) due to its amount was very small (500 μmol).

The SEM images of Fe<sub>2</sub>O<sub>3</sub>/CFB, CuO/CFB, and TiO<sub>2</sub>/CFB catalysts are exhibited in Figure 3. All the catalysts have rough surface morphology. The EDX results (Table 1) depict that all catalysts were dominated by many elements such as C, O, S, and Ca. The presence of Fe, Ti, and Cu are clearly observed in the EDX results. Figure 4 shows nitrogen adsorption-desorption isotherms of CFB, Fe<sub>2</sub>O<sub>3</sub>/CFB, CuO/CFB and TiO<sub>2</sub>/CFB. All isotherms of catalysts were Type IV in the IUPAC classifications, which are a typical isotherm for mesoporous materials. The isotherms of all catalysts exhibited clear hysteresis loops. The BET surface area, pore-volume, and mean pore size of CFB, Fe<sub>2</sub>O<sub>3</sub>/CFB, CuO/CFB, and TiO<sub>2</sub>/CFB were obtained from the nitrogen adsorption-desorption analysis. The complete data are listed in Table 2. The pore size distribution of CFB, Fe<sub>2</sub>O<sub>3</sub>/CFB, CuO/CFB, and TiO<sub>2</sub>/CFB indicates the presence of uniform mesopores such as 4.4, 10.2, 10.4, and 7.7 nm, respectively. The

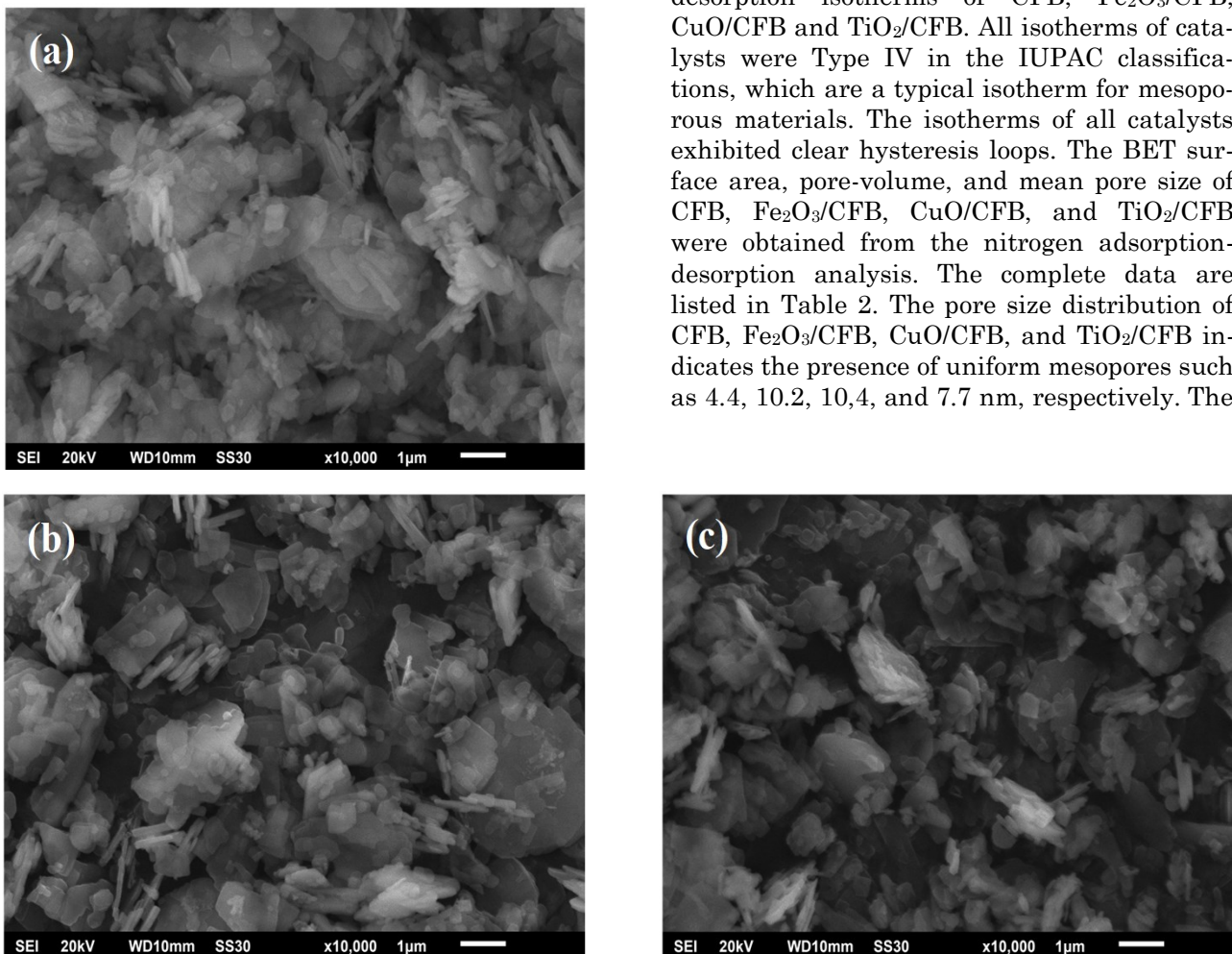


Figure 3. SEM images of (a) Fe<sub>2</sub>O<sub>3</sub>/CFB, (b) CuO/CFB and (c) TiO<sub>2</sub>/CFB.

Table 1. Physical properties of SEM EDX of the catalysts.

Element	Wt%		
	Fe <sub>2</sub> O <sub>3</sub> /CFB	CuO/CFB	TiO <sub>2</sub> /CFB
C	11.55	39.39	51.58
O	52.99	45.26	40.76
S	16.06	5.80	3.16
Ca	17.08	6.07	3.47
Ti	-	-	0.42
Fe	1.43	0.02	0.02
Cu	0.85	2.23	0.59
Zn	-	0.67	-
Zr	-	0.54	-

BET surface area and pore volume showed the following values:  $158.8 \text{ m}^2 \cdot \text{g}^{-1}$ ,  $0.350 \text{ cm}^3 \cdot \text{g}^{-1}$  for CFB;  $7.610 \text{ m}^2 \cdot \text{g}^{-1}$ ,  $0.039 \text{ cm}^3 \cdot \text{g}^{-1}$  for  $\text{Fe}_2\text{O}_3/\text{CFB}$ ;  $7.337 \text{ m}^2 \cdot \text{g}^{-1}$ ,  $0.038 \text{ cm}^3 \cdot \text{g}^{-1}$  for  $\text{CuO}/\text{CFB}$  and  $13.790 \text{ m}^2 \cdot \text{g}^{-1}$ ,  $0.053 \text{ cm}^3 \cdot \text{g}^{-1}$  for  $\text{TiO}_2/\text{CFB}$ , respectively. The complete data were shown in Table 2. It can be seen that the BET surface area and pore volume drastically decrease when CFB was modified to be catalysts by the impregnation process.

### 3.2. Catalytic Activity of Catalysts

The histogram of product yields from styrene oxidation with  $\text{H}_2\text{O}_2$  as oxidant catalyzed by  $\text{TiO}_2$ , CFB,  $\text{Fe}_2\text{O}_3/\text{CFB}$ ,  $\text{CuO}/\text{CFB}$ , and  $\text{TiO}_2/\text{CFB}$  catalysts are shown in Figure 5. The styrene conversion over blank (without cata-

lyst),  $\text{TiO}_2$ , CFB,  $\text{Fe}_2\text{O}_3/\text{CFB}$ ,  $\text{CuO}/\text{CFB}$  and  $\text{TiO}_2/\text{CFB}$  catalysts are 1.43; 3.16; 0.41; 11.59; 0.49 and 22.99%, respectively. If compared to  $\text{TiO}_2$  and CFB catalysts, the catalytic performance of  $\text{Fe}_2\text{O}_3/\text{CFB}$  (TON = 23.18) and  $\text{TiO}_2/\text{CFB}$  (TON = 45.98) catalysts are better than the others.

Titania and iron oxide on the surface of CFB was found as a suitable catalytic active site for the oxidation of styrene with aqueous  $\text{H}_2\text{O}_2$  as an oxidant. Otherwise, the catalytic performance of  $\text{CuO}/\text{CFB}$  is lower than  $\text{TiO}_2$  and almost the same with CFB catalyst support. It proves that the copper oxide was not active in the styrene oxidation with  $\text{H}_2\text{O}_2$  as an oxidant. This might due to the  $\text{H}_2\text{O}_2$  has adsorbed onto the catalytic surface of  $\text{CuO}/\text{CFB}$  but slow in  $\text{H}_2\text{O}_2$  decomposition to form  $\cdot\text{OH}$  radicals [19–21] It is demonstrated that, based on product conversion, the  $\text{TiO}_2/\text{CFB}$  catalyst is the best compared to the others. One considers that the  $\text{Ti}^{4+}$  in  $\text{TiO}_2/\text{CFB}$  catalyst has a higher amount of the electron vacancies in *d* orbital compared to  $\text{Fe}^{3+}$  and  $\text{Cu}^{2+}$ . So,  $\text{Ti}^{4+}$  ions in  $\text{TiO}_2/\text{CFB}$  catalyst can provide a large concentration of low energy electronic states and elec-

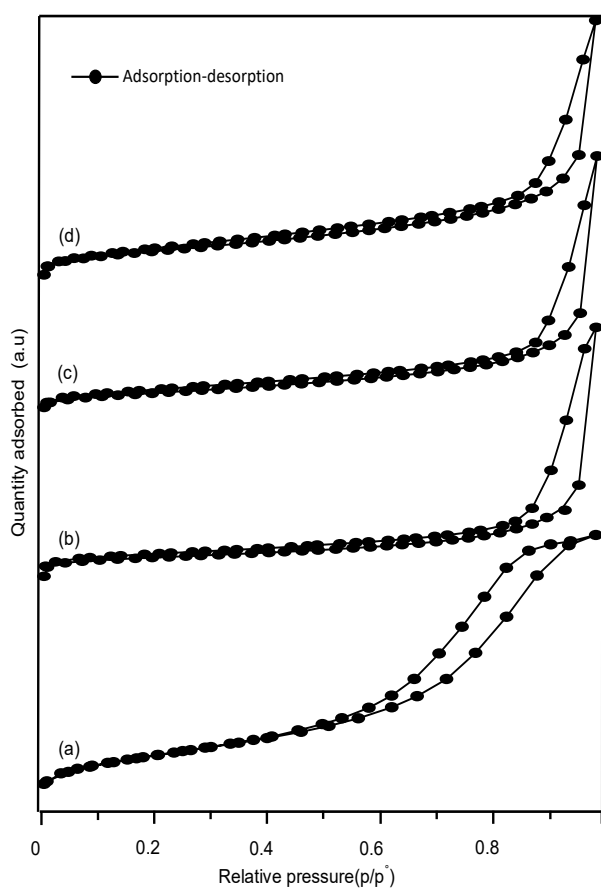


**Figure 4.** The physisorption isotherms of (a) CFB, (b)  $\text{Fe}_2\text{O}_3/\text{CFB}$ , (c)  $\text{CuO}/\text{CFB}$  and (d)  $\text{TiO}_2/\text{CFB}$ .

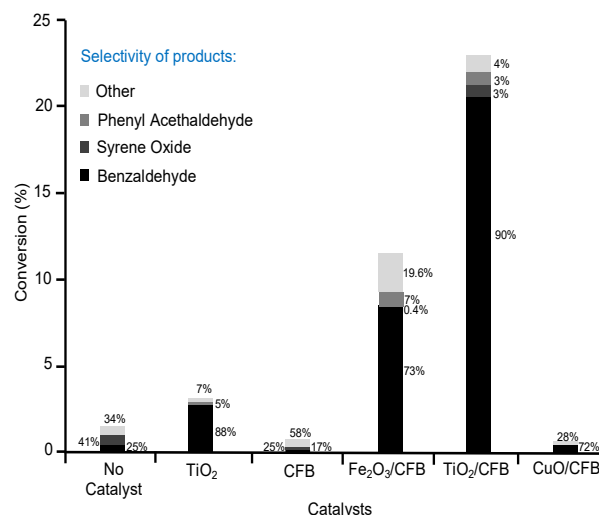


**Figure 5.** Comparison of catalytic performance of no catalyst,  $\text{TiO}_2$ , CFB,  $\text{Fe}_2\text{O}_3/\text{CFB}$ ,  $\text{TiO}_2/\text{CFB}$  and  $\text{CuO}/\text{CFB}$  catalysts in the oxidation of styrene (5 mmol), 30%  $\text{H}_2\text{O}_2$  (5 mmol) and catalyst (50 mg) at room temperature for 24 h.

**Table 2.** Physical properties of CFB,  $\text{Fe}_2\text{O}_3/\text{CFB}$ ,  $\text{CuO}/\text{CFB}$  and  $\text{TiO}_2/\text{CFB}$  catalysts.

Samples	BET surface area ( $\text{m}^2/\text{g}$ )	Pore Volume ( $\text{cm}^3/\text{g}$ )	Mean pore size (nm)
CFB	158.8	0.3500	4.41
$\text{Fe}_2\text{O}_3/\text{CFB}$	7.610	0.0386	10.16
$\text{CuO}/\text{CFB}$	7.337	0.0381	10.39
$\text{TiO}_2/\text{CFB}$	13.790	0.0532	7.70

tron vacancies states, so that it can facilitate the oxidation of styrene with  $H_2O_2$  [17]. It is also reported that the formation of the titanium peroxy complex plays a vital role in the higher catalytic activity of  $TiO_2/CFB$ . The peroxy complexes might undergo homolytic cleavage on O-OH to form  $\cdot OH$  radicals, which could further react with other  $H_2O_2$  to form  $O_2\cdot^-$  and  $\cdot OOH$  radicals. Thus,  $TiO_2/CFB$  is more reactive in the oxidation of styrene using  $H_2O_2$  [22]. By comparing  $Fe_2O_3/CFB$  and  $CuO/CFB$ , it is found that  $Fe_2O_3/CFB$  came before  $CuO/CFB$  because of  $CuO/CFB$  displays higher electronic configuration state and almost occupied electron vacancy state. The electronic configuration of  $Cu^{2+}$  is  $[Ar] 3d^9$ ; whereas  $Fe^{3+}$  is  $[Ar] 3d^5$ , which indicates that  $Fe^{3+}$  has more empty orbitals for substrate accommodation in conjuncture of its half-filled orbital is more stable for catalyzing a reaction.

The surface area is one of the essential factors to be considered for the higher catalytic activity of  $TiO_2/CFB$ . It is clearly observed that the  $TiO_2/CFB$  catalyst has the highest surface area compared to  $Fe_2O_3/CFB$  and  $CuO/CFB$  catalysts. Nonetheless, the surface area of CFB reduced tremendously after the impregnation of  $TiO_2$ ,  $CuO$  and  $Fe_2O_3$  respectively. It is owing to the particles size of those three metal oxides are too large and almost cover the surface and pore volume of CFB, proven by the mean pore size shown in Table 2. Table 2 shows the mean pore sizes of  $Fe_2O_3/CFB$  is 10.16 nm,  $CuO/CFB$

is 10.39 nm and  $TiO_2/CFB$  is 7.70 nm, are larger than mean pore size of CFB. By considering  $TiO_2/CFB$  has the highest surface area compared to metal oxides/CFB, it can be summarized that the catalytic performance of  $TiO_2/CFB$  evidences the important function of the active site and surface area of the catalyst. From the histogram, it can be seen that the styrene conversion of  $TiO_2$  (3.16%) and CFB (0.41%) increase drastically to be  $\sim 12\%$  and  $\sim 23\%$  when  $Fe_2O_3/CFB$  and  $TiO_2/CFB$  catalysts were used.

Benzaldehyde, phenyl acetaldehyde, and styrene oxide were the main products of styrene oxidation using  $H_2O_2$  as an oxidant. It reveals that the products are selective to the formation of benzaldehyde. The benzaldehyde selectivity of blank (no catalyst), CFB,  $TiO_2$ ,  $Fe_2O_3/CFB$ ,  $CuO/CFB$ , and  $TiO_2/CFB$  catalysts was 25.2; 17.4; 88.3; 73.2; 72.4 and 90.1%, respectively.

### 3.3 Kinetic Model: the Power-Rate Law

A series kinetic experiment of styrene oxidation by  $H_2O_2$  was carried out at room temperature with acetonitrile as solvent. The reaction mechanism scheme of styrene with  $H_2O_2$ , to produce benzaldehyde as the main product, is illustrated in Figure 6. This catalytic conversion reaction involves five steps: (1) At pre-equilibrium step,  $TiO_2/CFB$  reacts with  $H_2O_2$  to generate titanium(IV) hydroperoxy species; (2)

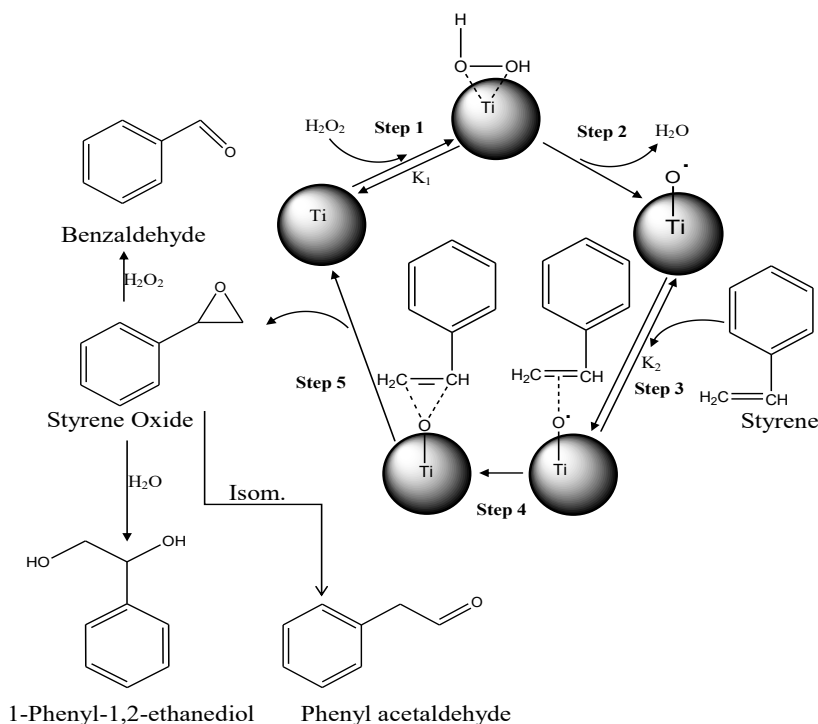


Figure 6. Reaction scheme of the styrene oxidation with  $H_2O_2$  as oxidant [23,24].

Titanium(IV) hydroperoxy species are unstable, thus re-arranging themselves to form titanium(IV) oxo radicals by releasing water molecules as the by-product; (3) The highly active titanium(IV) oxo radicals collide with styrene at the second pre-equilibrium state to give  $\pi$ -bonded transient species; (4) Titanium(IV) oxo radicals transfer its oxygen to styrene by giving metalloepoxy intermediate species; (5) Titanium(IV) species in TiO<sub>2</sub>/CFB regains its structure with the generation of styrene oxide. Since styrene oxide is an active intermediates, it can transform into several products, such as benzaldehyde (main product), 1-phenyl-1,2-ethanediol and phenyl acetaldehyde [23,24]. The proposed mechanism for the oxidation of styrene is consistent with the observation made in kinetic.

The kinetic model, such as: the power-rate law was used to best fit the results. The power-rate law can be represented as [25,26]:

$$r_i = -\frac{dC_i}{dt} = kK_1K_2[\text{catalyst}][\text{Styrene}][H_2O_2]^{1/2} \quad (1)$$

$$r_i = -\frac{d[C_0 - x]}{dt} = kK_1K_2[\text{catalyst}][\text{Styrene}][H_2O_2]^{1/2} \quad (2)$$

$$r_i = \frac{dx}{dt} = kK_1K_2[\text{catalyst}][\text{Styrene}][H_2O_2]^{1/2} \quad (3)$$

where  $r_i$  is the reaction rate of the styrene oxidation (mol.cm<sup>-3</sup>.s<sup>-1</sup>);  $k$  is the reaction rate constant (min<sup>-1</sup>);  $C_i$  is styrene concentration after oxidation time  $t$  (mol.cm<sup>-3</sup>); [catalyst] is concentration of TiO<sub>2</sub>/CFB catalyst and  $K_1$  and  $K_2$  are preequilibrium constants of the step in the Scheme. If the total catalyst concentration is expressed as [catalyst]<sub>T</sub> and considering the steady state approach, which includes the concentration of all the intermediate catalyst species, the power-rate law can be given as:

$$r_i = \frac{kK_1K_2[\text{catalyst}][\text{Styrene}][H_2O_2]^{1/2}}{1 + K_1[H_2O_2]^{1/2} + K_1K_2[\text{Styrene}][H_2O_2]^{1/2}} \quad (4)$$

$$\frac{[\text{catalyst}]_T}{r_i} = \frac{1 + K_1[H_2O_2]^{1/2} + K_1K_2[\text{Styrene}][H_2O_2]^{1/2}}{kK_1K_2[\text{Styrene}][H_2O_2]^{1/2}} \quad (5)$$

$$\frac{[\text{catalyst}]_T}{r_i} = \frac{1}{[\text{Styrene}]} \left\{ \frac{1}{kK_1K_2[H_2O_2]^{1/2}} + \frac{1}{kK_2} \right\} + \frac{1}{k} \quad (6)$$

The value of rate constant  $k$  was determined of the intercept from the plot of [catalyst]<sub>T</sub>/ $r_i$  vs 1/[styrene]. The kinetics data obtained from styrene oxidation with H<sub>2</sub>O<sub>2</sub> as oxidant onto TiO<sub>2</sub>/CFB are recorded in Table 3. Base on the experiment results, the styrene oxidation onto TiO<sub>2</sub>/CFB catalyst at room temperature obeys a first-order reaction model with the correlation coefficients R<sup>2</sup> ~ 0.9002 and the value of rate constant  $k = 0.00081 \text{ min}^{-1}$ .

#### 4. Conclusions

The use of carbon-derived fish bones (CFB) as catalyst support has been demonstrated in the styrene oxidation with aqueous H<sub>2</sub>O<sub>2</sub> in this research. It is found that the combination of titania (TiO<sub>2</sub>) and carbon-derived fish bones gave the highest catalytic activity compared to Fe<sub>2</sub>O<sub>3</sub>/CFB and CuO/CFB. The conversion and selectivity of styrene and benzaldehyde over TiO<sub>2</sub> was 3.16% and 88.3%; CFB is 0.41% and 17.4%; Fe<sub>2</sub>O<sub>3</sub>/CFB is 11.59% and 73.15%; CuO/CFB is 0.49% and 72.42%; and TiO<sub>2</sub>/CFB is 22.99% and 90.1%. The highest catalytic activity of TiO<sub>2</sub>/CFB was influenced by the electronic properties of Ti<sup>4+</sup> and the high surface area of the catalyst. The kinetic of styrene oxidation by H<sub>2</sub>O<sub>2</sub> fitted the first order with the rate constant  $k = 8.1 \times 10^{-4} \text{ min}^{-1}$ .

#### Acknowledgements

The authors gratefully acknowledge research grant from Kemenristek/BRIN Year 2020 and Islamic development bank (IsDB) contract number: 303/UN17.11/PL/2020, Universitas Mulawarman, East Kalimantan Province, Indonesia.

**Table 3.** First order kinetics of styrene oxidation onto TiO<sub>2</sub>/CFB catalysts.

Catalyst	Time (min)					First order	
	0	60	120	240	360	R <sup>2</sup>	k <sub>1</sub> (min <sup>-1</sup> )
$x$	0	0.0159	0.0201	0.0386	0.0465	0.9002	0.00081
$C_i$	0.8944	0.8785	0.8743	0.8558	0.8479		
TiO <sub>2</sub> /CFB	$\frac{\partial x}{\partial t}$	0	2.65 × 10 <sup>-4</sup>	1.675 × 10 <sup>-4</sup>	1.608 × 10 <sup>-4</sup>	1.291 × 10 <sup>-4</sup>	

(condition: 5mmol styrene = 0.5806 mL; 5mmol H<sub>2</sub>O<sub>2</sub> = 0.5107 mL; Acetonitrile = 4.5 mL and catalyst = 50 mg)

**References**

- [1] Ito, S., Kon, Y., Nakashima, T., Hong, D., Konno, H., Ino, D., Sato, K. (2019). Titania-Catalyzed H<sub>2</sub>O<sub>2</sub> Thermal Oxidation of Styrenes to Aldehydes. *Molecules*, 24(1), 1–9, doi: 10.3390/molecules24142520
- [2] Zhang, L.-X., Hua, Z.-L., Dong, X.-P., Li, L., Chen, H.-R., Shi, J.-L. (2007). Preparation of highly ordered Fe-SBA-15 by physical-vapor-infiltration and their application to liquid phase selective oxidation of styrene. *J. Mol. Catal. A Chem.*, 268, 155–162, doi: 10.1016/j.molcata.2006.12.027
- [3] Wang, H., Qian, W., Chen, J., Wu, Y., Xu, X., Wang, J., Kong, Y. (2014). Spherical V-MCM-48: the synthesis, characterization and catalytic performance in styrene oxidation. *RSC Advances*, 4, 50832–50839. doi: 10.1039/c4ra08333d
- [4] Yang, Y., Zhang, Y., Hao, S., Guan, J., Ding, H., Shang, F., Kan, Q. (2010). Heterogenization of functionalized Cu(II) and VO(IV) Schiff base complexes by direct immobilization onto amino-modified SBA-15: Styrene oxidation catalysts with enhanced reactivity. *Appl. Catal. A: General*, 381, 274–281, doi: 10.1016/j.apcata.2010.04.018
- [5] Li, B., Zhu, Y., Jin, X. (2015). Synthesis of cobalt-containing mesoporous catalysts using the ultrasonic-assisted “pH-adjusting” method: Importance of cobalt species in styrene oxidation. *J. Solid State Chem.*, 221, 230–239, doi: 10.1016/j.jssc.2014.10.008
- [6] Zhan, W., Guo, Y., Wang, Y., Guo, Y., Liu, X., Wang, Y., Lu, G. (2009). Study of Higher Selectivity to Styrene Oxide in the Epoxidation of Styrene with Hydrogen Peroxide over La-Doped MCM-48 Catalyst. *J. Phys. Chem. C*, 113(17), 7181–7185, doi:10.1021/jp8101095
- [7] Zou, H., Xiao, G., Chen, K., Peng, X. (2018). Noble metal free V<sub>2</sub>O<sub>5</sub>/g-C<sub>3</sub>N<sub>4</sub> composite for selective oxidation of olefins using hydrogen peroxide as oxidant. *Dalton Transactions*, 47, 13565–13572, doi: 10.1039/C8DT02765J
- [8] Zou, H., Hu, C., Chen, K., Xiao, G., Peng, X. (2018). Cobalt Vanadium Oxide Supported on Reduced Graphene Oxide for the Oxidation of Styrene Derivatives to Aldehydes with Hydrogen Peroxide as Oxidant. *Synlett*, 29, 2181–2184, doi: 10.1055/s-0037-1610630
- [9] Shi, F., Tse, M. K., Pohl, M.-M., Brückner, A., Zhang, S., Beller, M. (2007). Tuning Catalytic Activity between Homogeneous and Heterogeneous Catalysis: Improved Activity and Selectivity of Free Nano-Fe<sub>2</sub>O<sub>3</sub> in Selective Oxidations. *Angew. Chem. Int. Ed.*, 46, 8866–8868, doi: 10.1002/anie.200703418
- [10] Xie, L., Wang, H., Lu, B., Zhao, J., Cai, Q. (2018). Highly selective oxidation of styrene to benzaldehyde over Fe<sub>3</sub>O<sub>4</sub> using H<sub>2</sub>O<sub>2</sub> aqueous solution as oxidant. *React. Kinet. Mech. Catal.*, 125, 743–756, doi: 10.1007/s11144-018-1429-6
- [11] Milovac, D., Weigand, I., Kovačič, M., Ivanković, M., Ivanković, H. (2018). Highly porous hydroxyapatite derived from cuttle fish bone as TiO<sub>2</sub> catalyst support. *Proc. Appl. Ceram.*, 12(2), 136–142, doi: 10.2298/PAC1802136M
- [12] Puma, G.L., Bono, A., Krishnaiah, D., Collin, J.G. (2008). Preparation of titanium dioxide photocatalyst loaded onto activated carbon support using chemical vapor deposition: A review paper. *J. Hazard. Mater.*, 157, 209–219, doi: 10.1016/j.jhazmat.2008.01.040
- [13] Nurhadi, M., Chandren, S., Yuan, L.S., Ho, C.S., Mahlia, T.M.I., Nur, H. (2017). Titania-Loaded Coal Char as Catalyst in Oxidation of Styrene with Aqueous Hydrogen Peroxide. *Int. J. Chem. Reactor Eng.*, 15(1), 1–11, doi: 10.1515/ijcre-2016-0088
- [14] Nurhadi, M. (2017). Modification of Coal Char-loaded TiO<sub>2</sub> by Sulfonation and Alkylsilylation to Enhance Catalytic Activity in Styrene Oxidation with Hydrogen Peroxide as Oxidant. *Bull. Chem. React. Eng. Catal.*, 12(1), 55–61, doi: 10.9767/bcrec.12.1.501.55-61
- [15] Kusumawardani, R., Nurhadi, M., Wirhanuddin, Gunawan, R., Nur, H. (2019). Carbon-containing Hydroxyapatite Obtained from Fish Bone as Low-cost Mesoporous Material for Methylene Blue Adsorption. *Bull. Chem. React. Eng. Catal.*, 14(3), 660–671, doi: 10.9767/bcrec.14.3.5365.660-671
- [16] Nurhadi, M. (2017). utilization Low Rank Coal Bottom Ash as TiO<sub>2</sub> Support for Oxidation Catalyst of Styrene with Hydrogen Peroxide Aqueous. *Key Eng. Mater.*, 733, 12–16, doi: 10.4028/www.scientific.net/KEM.733.12
- [17] Gheisari, H., Karamian, E., Abdollahi, M. (2015). A novel hydroxyapatite–Hardystonite nanocomposite ceramic. *Ceram. Int.*, 41(41), 5967–5975, doi: 10.1016/j.ceramint.2015.01.033
- [18] Słocarczyk, A., Paszkiewicz, Z., Paluszkiwicz, C. (2005). FTIR and XRD evaluation of carbonated hydroxyapatite powders synthesized by wet methods. *J. Mol. Struct.*, 744–747, 657–661, doi: 10.1016/j.molstruc.2004.11.078
- [19] Zhang, L., Yuan, F., Zhang, X., Yang, L. (2011). Facile synthesis of flower like copper oxide and their application to hydrogen peroxide and nitrite sensing. *Chem. Central J.*, 5, 75, doi: 10.1186/1752-153X-5-75



- [20] Lousada, C.M., Yang, M., Nilsson, K., Jonsson, M. (2013). Catalytic decomposition of hydrogen peroxide on transition metal and lanthanide oxides. *J. Mol. Catal. A Chem.*, 379, 178–184, doi: 10.1016/j.molcata.2013.08.017
- [21] Liou, R.-M., Chen, S.-H. (2009). CuO impregnated activated carbon for catalytic wet peroxide oxidation of phenol. *J. Hazard. Mater.*, 172, 498–506, doi: 10.1016/j.jhazmat.2009.07.012.
- [22] Lousada, C.u.M., Johansson, A.J., Brinck, T., Jonsson, M. (2012). Mechanism of H<sub>2</sub>O<sub>2</sub> Decomposition on Transition Metal Oxide Surfaces. *J. Physic. Chem. C*, 116, 9533–9543, doi: 10.1021/jp300255h
- [23] Lubis, S., Yuliaty, L., Lee, S. L., Sumpono, I., Nur, H. (2012). Improvement of catalytic activity in styrene oxidation of carbon-coated titania by formation of porous carbon layer. *Chem. Eng. J.*, 209, 468–493, doi: 10.1016/j.cej.2012.08.041
- [24] Indira, V., Halligudi, S.B., Gopinathan, S., Gopinathan, C. (2001). Kinetics and Mechanism of Styrene Oxidation Using Transition Metal Substituted Dodecatungstophosphate. *React. Kinet. Catal. Lett.*, 73(1), 99–107, doi: 10.1023/A:1013985123468
- [25] Pei, J., Han, X., Lu, Y. (2015). Performance and kinetics of catalytic oxidation of formaldehyde over copper manganese oxide catalyst. *Build. Environ.*, 84, 134–141, doi: 10.1016/j.buildenv.2014.11.002
- [26] Tseng, T.K., Chu, H. (2001). The kinetics of catalytic incineration of styrene over a MnO-FeO catalyst. *Scien. Total Environ.*, 275, 83–93, doi: 10.1016/S0048-9697(00)00856-1